INDUCTION MOTOR EFFICIENCY ESTIMATION UNDER NON-SINUSOIDAL SUPPLY CONDITION

Aminu, M.

Department of Electrical and Electronics Engineering, Modibbo Adama University, Yola, Adamawa State, Nigeria

Corresponding Email: aminumhd@mautech.edu.ng

ABSTRACT

Several methods have been proposed in literature for the estimation of induction motor efficiency under sinusoidal supply condition. However, only a few of those methods can be considered suitable for motors operating under distorted or non-sinusoidal supply condition. In this paper a new method is proposed for induction motor efficiency estimation under non-sinusoidal supply conditions - to take into account the presence of harmonics in the power supply. By using a modified equivalent circuit approach, the method considers the variations of the core loss resistance due to time harmonics. Also, the changes in the rotor bar resistance and the leakage inductance due to skin effects at higher frequencies is considered in the harmonic equivalent circuit. Two induction motors of different design classifications are tested to validate the proposed method under different levels of voltage unbalance and harmonics conditions. These two motors are a 37kW standard efficiency and a 7.5kW premium efficiency induction motors. Finally, the efficiency estimation via the proposed method is compared to the IEC60034-2-3 standard in the case of a balanced non-sinusoidal supply condition. This allows not only the efficiency comparison but also the loss segregation analysis on the various components of the motor losses. In the case of an unbalanced supply, the efficiency results are compared to measured values obtained via the direct input-output method. The results obtained indicate that the maximum absolute efficiency errors at 9.96% THD_v for the 7.5kW and 37kW test motors were found to be 0.234% and 0.248% respectively. These values confirm the accuracy of the proposed method.

Keywords: Efficiency Estimation, Non-Sinusoidal Supply, Unbalanced Supply, Harmonics, Equivalent Circuit.

1 INTRODUCTION

Induction machines play a vital role in our day-to-day life. It is one of the most widely used machines in industries due to its simplicity, robustness, reliability, high efficiency and low cost. Additional losses are incurred by induction motors when operated with non-sinusoidal or distorted power supply due to the presence of harmonics. With the rapid development in power electronics and the advances in motor control strategies, variable frequency drives (VFDs) have become very popular in industrial applications. While there are several benefits that come with the use of VFDs, their outputs are not purely sinusoidal but rather a superposition of sinusoidal waves with frequencies that are multiples of the fundamental network frequency. These superimposed waveforms are termed as harmonics in the system. The harmonics generally exhibited by induction motors are of two types, namely: space harmonics and time harmonics [1]. The space harmonics in a motor driven by a sinusoidal supply is caused by the non-sinusoidal distribution of the mmf produced in the air gap and the magnetic interaction of the different phase windings [1]. Time harmonics are as a result of power supply distortions [1, 2]. The harmonic currents produce rotating fields in the air gap that rotate at higher speeds than the rotating fundamental field [2]. The presence of harmonics significantly affects the operation of induction motors. More notably is the increase in copper and core losses [3].

In terms of the copper losses, the additional losses come from the increase in the rms values of the stator currents and stator winding resistance due to the higher operating temperature of the VFD or distorted power supply [4]. The core loss, comprising of the hysteresis and eddy current losses (both of which are frequency dependant) are directly affected by the presence of low order harmonics in the power supply. While there are several methods that allow for the estimation of induction motor efficiency, only a few of those methods can be considered for motors operating under distorted or non-sinusoidal supply condition. One of the methods is the airgap torque method in which the airgap power is estimated based on the voltage and current waveforms [5]. However, in the AGT method, the mechanical and core loss are not accounted for, hence, an assumed fixed percentage value is used. This may have an impact on the accuracy of the method particularly for the non-sinusoidal supply since the presence of harmonics directly affect the core loss due to its dependence on frequency. The equivalent circuit method in conjunction with optimization techniques have been used for solving the efficiency estimation problem in the presence of harmonics in power supply as clearly demonstrated in [6, 7, 8]. However, the impact of the non-sinusoidal supply on the rotor and core loss resistances has not been taken into consideration. By using a modified equivalent circuit approach, the method proposed in this paper considers the variations of the core loss resistance due to time harmonics and the changes in the rotor bar resistance and the leakage inductance due to skin effects at higher frequencies.

2 MATERIALS AND METHODS

The operation of an induction motor under unbalanced non-sinusoidal supply conditions can be represented by three distinct equivalent circuits as shown in Figure. 1a to 1c. The positive and negative sequence equivalent circuits represent the unbalanced condition while the harmonic equivalent circuit represents the non-sinusoidal supply condition. Note that p and n subscripts in Figure 1(a) and 1(b) refer to the positive and negative sequence. The harmonic slip s_h in Figure 1(c) is as given by (1) where the positive and negative signs refer to the forward and backward rotating harmonics respectively. In Figure 1(c), the rotor and core loss resistances are considered to vary with the harmonics order, therefore, they are estimated separately for each harmonic equivalent circuit. The negative and positive signs in equation (1) represent the forward and backward rotating harmonics respectively.

$$s_h = \frac{hn_1 \mp n}{hn_1} \tag{1}$$

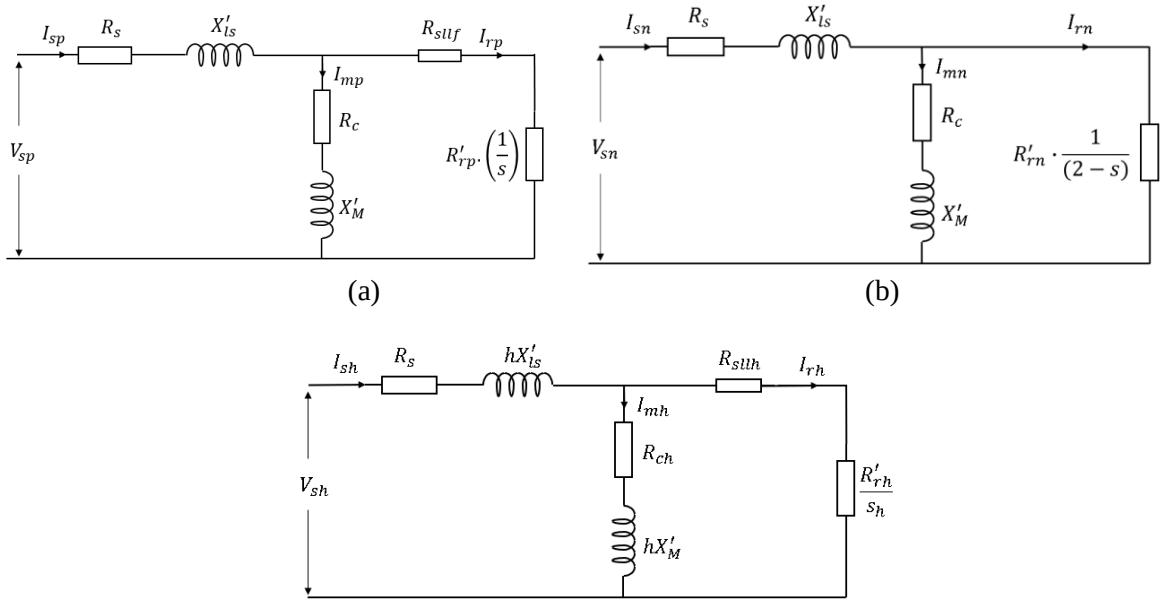

Figure 1. Induction motor equivalent circuit under unbalanced non-sinusoidal supply voltages (a) Positive sequence equivalent circuit (b) Negative sequence equivalent circuit (c) Harmonic equivalent circuit

The proposed algorithm for induction motor efficiency estimation when operating with non-sinusoidal supply is presented in the flowchart shown in Figure 2. The main steps involved in the proposed method are discussed as follows:

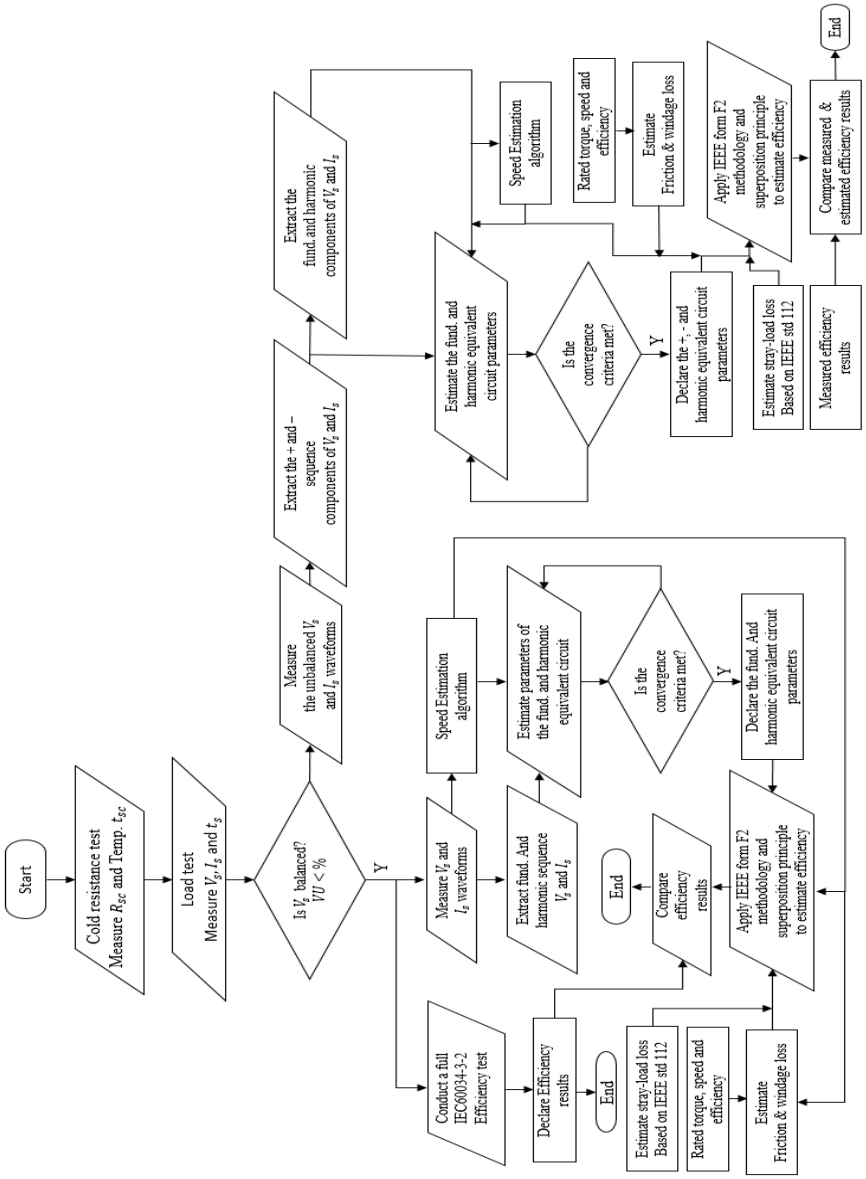

Figure 2. A Complete Flowchart of the Efficiency Estimation Algorithm in the Presence of Unbalance and Harmonics Supply

2.1 Harmonic and Sequence Component Extraction

From the measured stator line-to-line voltages and line currents signals, the phase sequence voltages (V_{sp} and V_{sn}) and currents components (I_{sp} and I_{sn}) for the positive and negative sequence equivalent circuits are determined. Under normal operation, the harmonics produced by a 6-pulse inverter are the odd, non-triple harmonics [2]. For an induction motor, the magnitudes of the harmonics diminish above the 17th order [9]. In this study, it was observed that the extracted harmonic voltage magnitudes for the tested motors become negligible by the 13th order, Hence, for simplicity, this study considers the distinct harmonic voltages of order 5^{th}, 7^{th}, 11^{th} and 13^{th} for the non-sinusoidal supply analysis. The harmonic signals imposed on the fundamental are generated using a programmable power supply unit. The waveform signals extracted from the supply unit serve as inputs to the parameter identification algorithm as demonstrated in the next section.

2.2 Parameter Identification

Two steps are followed in estimating the equivalent circuit parameters as demonstrated in Figure 3. The first step involved estimating the parameters of the fundamental equivalent circuit by solving for the optimal parameter vector θ through minimizing the least-square problem defined as follows:

$$\hat{\theta} = \underset{\theta \in [\theta_{min}, \theta_{max}]}{arg\,min} \quad F_{err}(\theta) \tag{2}$$

Where $F_{err}(\theta)$ is the sum-squared difference between the measured and estimated positive and negative sequence currents (obtained based on Figure 1a and 1b) as defined by equation (3).

$$F_{err}(\theta) = \sum_{j=1}^{N} \left(\left(\tilde{I}_{sp}(j) - \tilde{I}'_{sp}(j) \right)^2 + \left(\tilde{I}_{sn}(j) - \tilde{I}'_{sn}(j) \right)^2 \right) \tag{3}$$

Where θ is a vector set of the motor fundamental parameters. $\theta = \left[R'_{rp}, R_c\ X'_{lr}\ X'_m \right]^T$ for a balanced supply and $\theta = \left[R'_{rp}, R'_{rn}, R_c, X'_{lr}\ X'_m \right]^T$ for unbalanced supply, θ_{min} and θ_{max} are the lower and upper boundaries of the constraints respectively, the current sets $\tilde{I}_{sp}$, $\tilde{I}'_{sp}$ and $\tilde{I}_{sn}$, $\tilde{I}'_{sn}$ are the measured and estimated symmetrical component currents in the stator respectively, j is the data sample index and N is the total number of data samples. The second step involves the identification of the harmonic equivalent circuit parameters. Due to their dependence on frequency, the rotor and core loss resistances are set as unknown parameters for each harmonic order. The least-square minimization problem is therefore defined as follows:

$$\hat{\theta} = \underset{\theta \in [\theta_{min}, \theta_{max}]}{arg\,min} \ f_{err}(\theta) \tag{4}$$

Where $f_{err}(\theta)$ given in equation (5) is the sum-squared difference between the measured and estimated harmonic currents (based on Figure 1c).

$$f(\theta) = \sum_{j=1}^{n} \left(\left(\tilde{I}_{sh}(j) - \tilde{I}'_{sh}(j) \right)^2 \right) \tag{5}$$

The parameter vector in this case, is given by $\theta = [R'_{rh}, R_{ch}\ ]^T$, where h is the harmonic order. The forward and backward slips are calculated according to equation (1). The harmonic order associated with the forward and backword fields as shown in Table 1. Note that the speed, friction and windage loss and temperature estimation are all based on the IEEE Std. 112 methods [10].

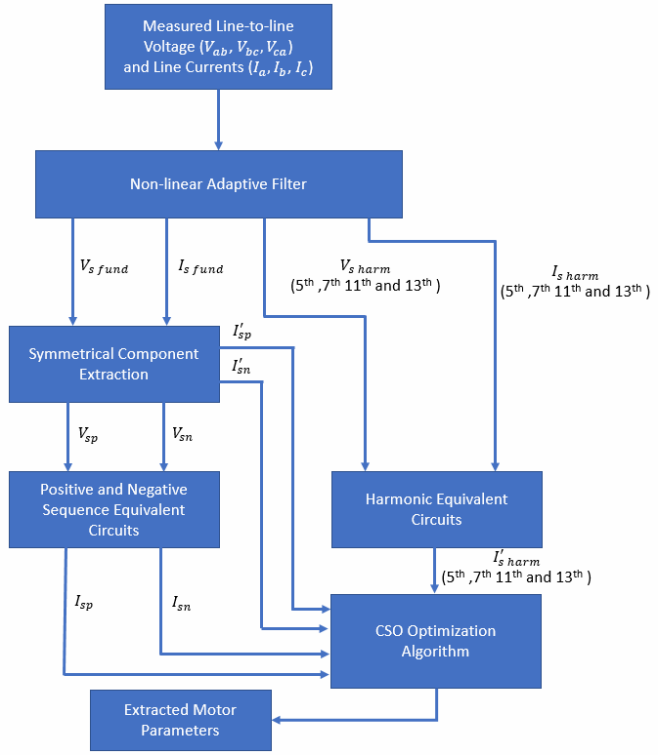

Figure 3. Induction motor parameter estimation scheme under balance/unbalanced non-sinusoidal supply

Table 1. Harmonics order associated with the forward and backward rotating field

k	Forward rotating harmonics order $h = 6k + 1$	Backward rotating harmonics order $h = 6k - 1$
1	7	5
2	13	11

2.3 Efficiency Calculation

The superposition principle is applied to calculate the power developed by the positive, negative and harmonics equivalents circuits. The motor efficiency using the proposed equivalent circuit approach is computed as follows:

$$\eta = \frac{P_{out}}{P_{in}} = \frac{(P_{dev-p} + P_{dev-n} + \sum_{h=5}^{13} P_{dev-h}) - P_{fw}}{P_{in}} \cdot 100\% \quad (6)$$

Where P_{dev-p} is the power developed by the positive sequence; P_{dev-n} is the power developed by the negative sequence; P_{dev-h} is the power developed by the harmonics; h is nontriplet odd harmonics ranging from the 5th to the 13th harmonic order; P_{fw} is the friction and windage loss; P_{in} is the input power which is calculated from the instantaneous voltages and current using (7).

$$P_{in} = v_a i_a + v_b i_b + v_c i_c = v_{ca}(i_a + i_b) - v_{ab} i_b \quad (7)$$

3 RESULTS AND DISCUSSION

Two induction motors of different design classifications were tested to validate the proposed NFEE method under different levels of voltage unbalance and harmonics conditions. These two motors are a 37kW standard efficiency and a 7.5kW premium efficiency induction motors. The nameplate data and experimental test rig used in testing these motors are as reported in Table 2.

Figure 4 respectively. The experimental tests were performed under two different operating scenarios: Case 1 for a balanced non-sinusoidal supply condition and Case 2 for a combination of different VU and THD levels.

Table 2. Nameplate Data of the Induction Motors used for Validation

Motor Efficiency class	7.5kW Motor Premium Eff.	37kW Motor Standard Eff.
Voltage (V)	380	400
Current (A)	14.4	67.4
Frequency (Hz)	50	50
Speed (rpm)	1460	1475
Power factor	0.88	0.86
Insulation class	F	F
Number of poles	4	4
Stator connection	Δ	Δ

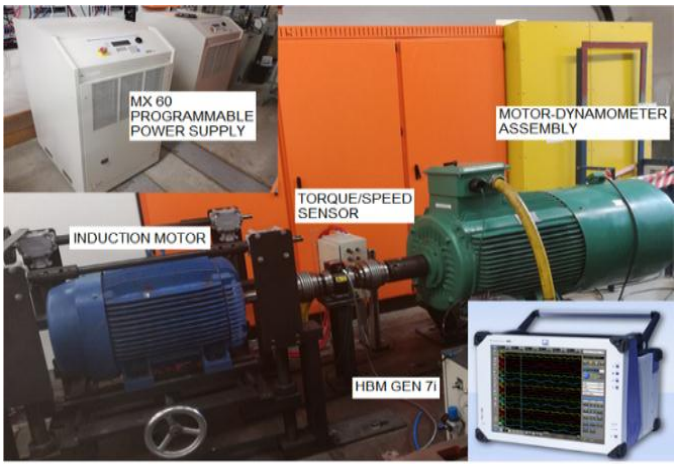

Figure 4. The complete 110kW laboratory test bench showing all the system components

3.1 Case 1: Balanced Non-sinusoidal Supply Condition

Firstly, the stator cold resistance test was performed to determine the stator resistance and the ambient temperature prior to starting the test. A rated load test was then performed to heat up the motor to its thermal equilibrium point. As specified by the IEC 60034-2-1 [11], the thermal equilibrium point is attained when the temperature change in 1 hour is less than 2K. The temperature at the thermal equilibrium point was recorded. This test was followed immediately by a load curve test at four different operating points (OP), ie, 100% (rated), 75%, 50% and 25%. It is important to emphasize that the motor parameters for the NFEE method were determined based on a single load point test. Hence, the essence of the load tests at different operating points is to compute the motor reference efficiencies according to the IEC60034-2-3 loss segregation procedure. The tests could also be helpful to verify the consistency of the parameter estimation method under different loading conditions. The tests were performed fast enough to ensure that the temperature variation remains within 5K as recommended by the IEC60034-2-1. The total voltage harmonic index THD_v in each test point was varied within the range of 10% down to 2% at an interval of 2%. The essence of using high VU level (exceeding the 5% limit set by the IEEE Std. 112 for sinusoidal supply) is to assess more distinctly the impact of the harmonics on the motor efficiency. The programmable power supply (MX60) was used to generate the required voltage harmonics and to ensure a balanced supply condition. The harmonic voltage magnitude associated with each harmonic order was added to the fundamental to give the required THD_v value as shown in Table 3. For data acquisition, the *Genesis 7i* Data Acquisition unit from HBM was used. This system has up to 24 DAQ channels and allows the synchronous acquisition of raw data from all the channels.

Table 3. Measured Data for Case 1 (Balanced Non-sinusoidal Condition)

$THD_v(\%)$	$V_{s-5^{th}}(V)$	$V_{s-7^{th}}(V)$	$V_{s-11^{th}}(V)$	$V_{s-13^{th}}(V)$
9.96	28.94	20.68	14.01	11.34
7.97	23.15	16.54	11.21	9.07
6.04	17.54	12.53	8.49	6.87
3.98	11.58	8.27	5.6	4.54
1.99	5.79	4.14	2.80	2.27

In addition to the measured data for calculating the reference motor efficiency using the loss segregation method, the voltage and current signal waveforms were recorded for each operating point at a sampling rate of 50kHz and a window length of 2s. Figure 5a and 5b show zoomed portions of the voltage and current waveforms recorded at the rated operating condition (OP4) with a 10% THD_v value.

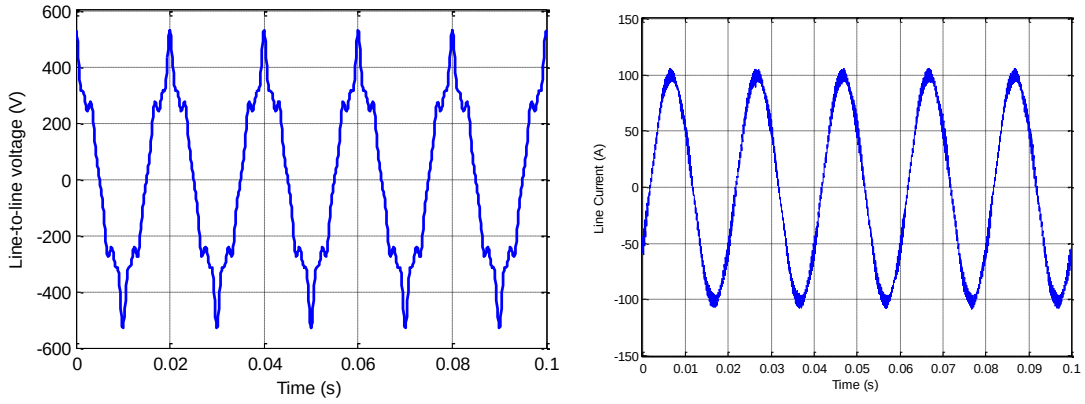

(a) (b)

Figure 5. Recorded stator signals at OP4 for the 37kW test motor (a) line-to-line voltage signal (b) Line current signal

To estimate the motor equivalent circuit parameters, the recorded voltage and current waveforms were passed through the adaptive non-linear filter to extract the fundamental and harmonic signal waveforms which serve as inputs to the parameter identification routine using the CSO algorithm. The estimated parameters at two different operating points as reported in Table 4 clearly indicate the consistency of the parameter estimation scheme. Hence, measurements from one single operating point is enough to extract all the motor parameters.

Table 4. Estimated Motor Parameters for the Fundamental and Harmonic Equivalent Circuits using CSO Algorithm

EC	Parameter	Motor parameters 7.5kW		Motor parameters 37kW	
		OP2 (50%)	OP4 (100%)	OP2 (50%)	OP4 (100%)
Fund.	$R'_{rp}(\Omega)$	0.640	0.642	0.144	0.148
	$X'_{ls}\ (\Omega)$	3.260	3.258	0.791	0.806
	$X'_{m}(\Omega)$	63.294	63.300	26.985	26.962
	$R_{c}(\Omega)$	2.538	2.579	0.302	1.315
Harm.	$R'_{r,\,5^{th}}(\Omega)$	1.346	1.399	0.263	0.265
	$R'_{r,\,7^{th}}(\Omega)$	1.402	1.405	0.271	0.276
	$R'_{r,\,11^{th}}(\Omega)$	1.445	1.448	0.276	0.285
	$R'_{r,\,13^{th}}(\Omega)$	1.529	1.533	0.308	0.321
	$R'_{c,\,5^{th}}(\Omega)$	2.673	2.716	1.375	1.385
	$R'_{c,\,7^{th}}(\Omega)$	2.735	2.779	1.470	1.417
	$R'_{c,\,11^{th}}(\Omega)$	2.810	2.855	1.406	1.456
	$R'_{c,\,13^{th}}(\Omega)$	2.835	2.881	1.454	1.469

Figure 6a and 6b show the profiles of the estimated rotor and core loss resistances corresponding to the fundamental and harmonic equivalent circuits. These results confirm the variations of these parameters with the order of the harmonics and therefore highlight the need to estimate the parameters separately using the harmonic equivalent circuits.

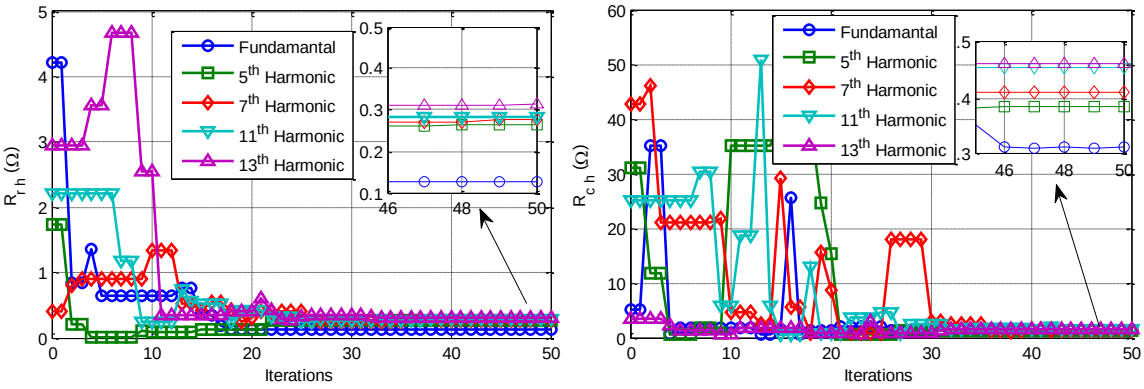

Figure 6. Estimation of the rotor and core loss resistances corresponding to each harmonic order at OP4 (a) Rotor resistance (b) Core loss resistance

With the estimated equivalent circuit parameters, the additional losses due to the harmonic supply can be determined based on the segregation of loss method. The results shown in Figure 7a to 7c are estimated at the worst THD_v of 10% for the 37kW motor. It is seen that the losses (including the load-dependent copper losses) show fairly constant values for all loading conditions and quite

significant dependence on the harmonics order. While the core loss as seen in Figure 7c is more noticeable for low order harmonics (especially the 5th order harmonic), the trend shows a reduction in the core loss for the higher order harmonics.

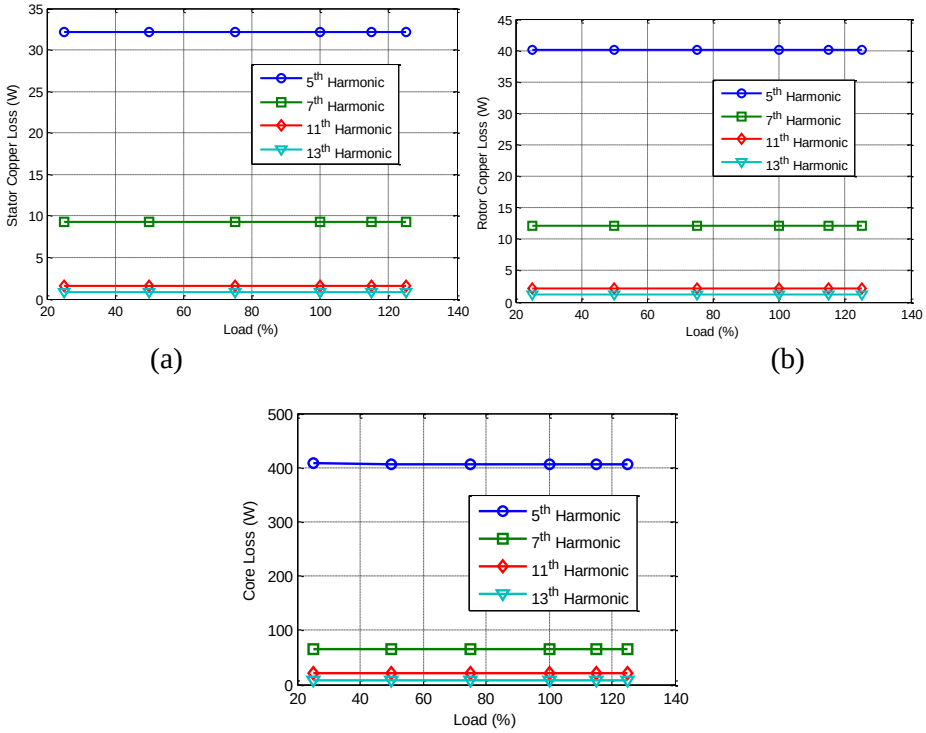

Figure 7. Stator and rotor copper losses and core loss due to harmonic at 10% THD_v (a) Stator copper loss (b) Rotor copper loss (c) Core loss

By comparing the estimated efficiencies of the tested motors at the lowest and highest THD_v for rated condition as shown in Figure 8a and 8b, it is seen that the 7.5 kW motor efficiency drops significantly by about 1.645% when operated with 9.96% THD_v. This contrasts with the 37kw motor which records only about 0.436% efficiency drop.

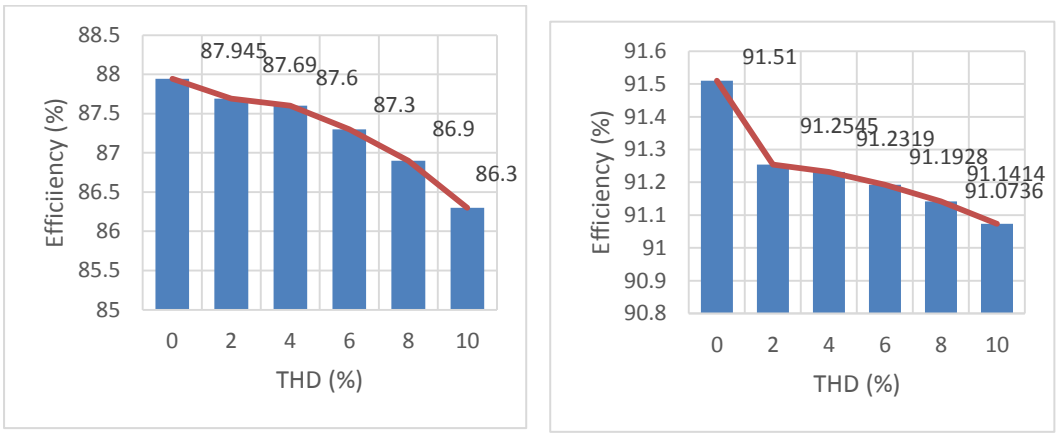

Figure 8. Estimated efficiency values at different THD_v levels (a) 7.5kW motor (b) 37kW motor

This disparity could be explained by the difference in how the losses are distributed within the two motors with respect to their design [12]. For the two tested motors, the results as shown in Figure 9 and 10 indicate that the predominant disparity in the losses appear to be the core loss, while the stray-load loss remains practically less impacted by the non-sinusoidal supply.

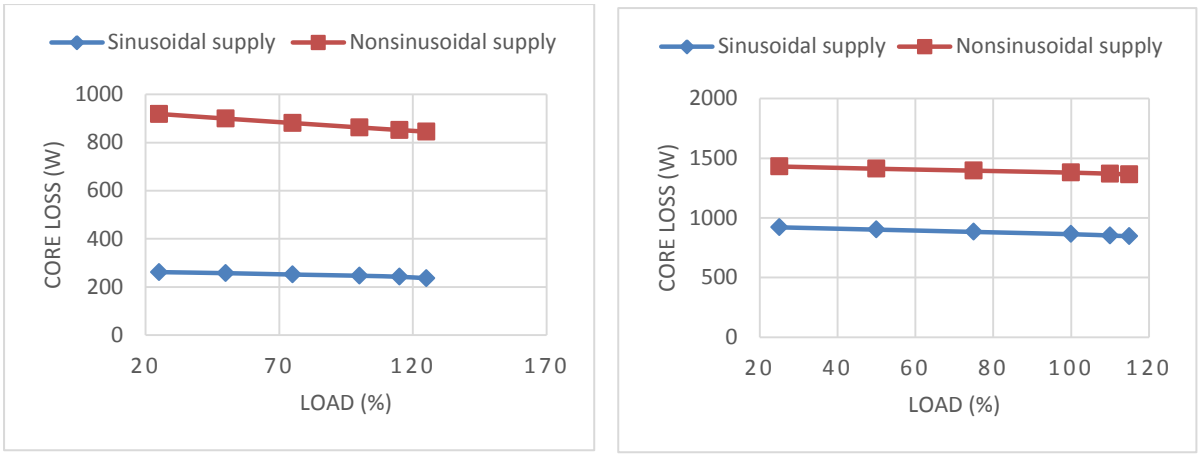

(a) (b)

Figure 9. Core loss estimation for sinusoidal and non-sinusoidal supplies (a) 7.5kW test moor (b) 37kW test motor

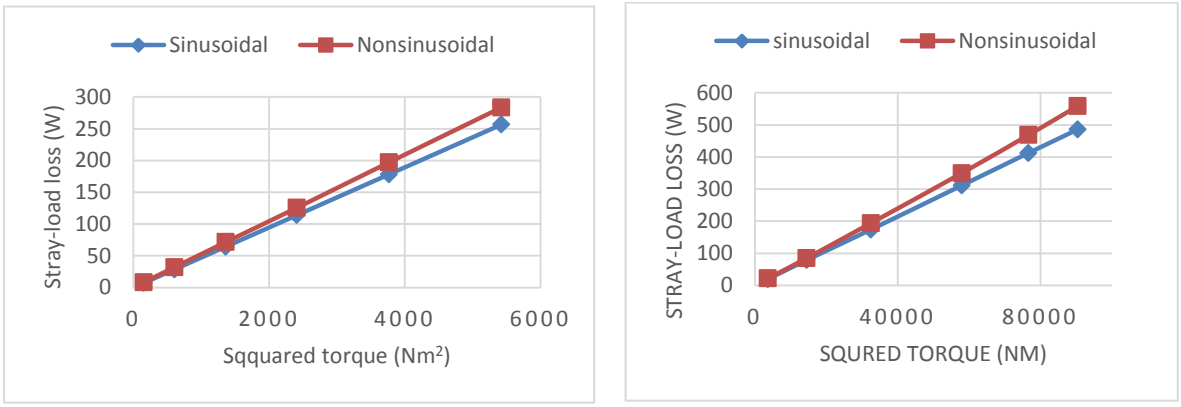

(a) (b)

Figure 10. Stray-load loss estimation for sinusoidal and non-sinusoidal supplies (a) 7.5kW test moor (b) 37kW test motor

The estimated and measured efficiency profiles at different THD_v and load levels for the 37kW motor is shown in Figure 11. The absolute errors between the measured and estimated efficiencies as summarized in Table 5 show that the maximum absolute error is 0.248% at 0.5% THD_v. This value indicates an acceptable level of accuracy by the proposed method.

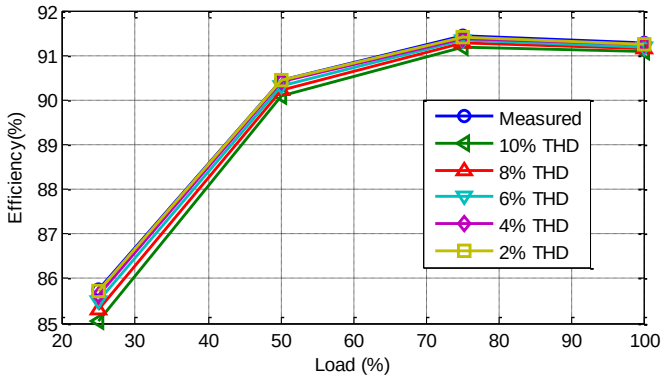

Figure 11. Estimated and measured efficiency profiles at different THD_v and load levels for 37kW motor

Table 5. Measured and Estimated Motor Efficiencies at Different THD_v values under Rated Operating Condition

THD_v (%)	7.5kW			37kW		
	Measured Efficiency (%)	Estimated Efficiency (%)	Abs. Error (%)	Measured Efficiency (%)	Estimated Efficiency (%)	Abs. Error (%)
0.50	87.698	87.945	0.248	91.420	91.510	0.090
1.99	87.502	87.690	0.187	91.361	91.254	0.106
3.98	87.457	87.600	0.143	91.364	91.232	0.132
6.04	87.202	87.300	0.097	91.398	91.193	0.206
7.97	86.786	86.900	0.114	91.266	91.141	0.125
9.96	86.199	86.300	0.101	91.262	91.074	0.188

3.2 Case 2: Unbalanced Non-sinusoidal Supply Condition

The test motors are subjected to different levels of voltage conditions with VU factor ranging from 1% to 5%. For each VU, the THD_v was varied within the range of 2% to 10% at an interval of 2%, and measurements were taken at each test point. The measured and estimated efficiency results corresponding to each test point are compared and the absolute errors are determined as shown in Table 6. The proposed method provides results with acceptable accuracies as the maximum absolute errors for the 7.5kW and 37kW motors are 0.3886% and 0.2480% respectively. It can be observed that the efficiencies drop significantly by 3.387% and 2.329% for the 7.5kW and 37kW motor respectively when the motors operate with a combination of both 5% VU and 10% THD_v.

Table 6. Measured and Estimated Motor Efficiencies at Different VU and THD_v values under Rated Operating Condition

VU (%)	THD_v (%)	7.5kW			37kW		
		Measured Efficiency (%)	Estimated Efficiency (%)	Absolute Error (%)	Measured Efficiency (%)	Estimated Efficiency (%)	Absolute Error (%)
1	1.99	87.500	87.688	0.188	91.352	91.245	0.107
	3.98	87.450	87.593	0.143	91.356	91.222	0.134
	6.04	87.193	87.291	0.098	91.391	91.185	0.206
	7.97	86.777	86.891	0.114	91.257	91.133	0.124
	9.96	86.190	86.291	0.101	91.253	91.065	0.188
2	1.99	86.206	86.234	0.128	91.244	91.038	0.207
	3.98	86.115	86.182	0.067	91.193	90.986	0.207
	6.04	86.033	86.130	0.096	91.141	90.935	0.206
	7.97	85.892	86.077	0.185	91.090	90.883	0.206

	9.96	85.800	86.025	0.224	91.038	90.832	0.206
3	1.99	85.666	85.924	0.257	90.835	90.634	0.201
	3.98	85.532	85.822	0.290	90.631	90.437	0.194
	6.04	85.398	85.721	0.323	90.427	90.239	0.188
	7.97	85.265	85.620	0.355	90.224	90.042	0.182
	9.96	85.130	85.519	0.389	90.021	89.844	0.177
4	1.99	85.093	85.307	0.214	89.719	89.476	0.243
	3.98	84.901	85.096	0.196	89.618	89.394	0.225
	6.04	84.827	84.986	0.159	89.517	89.343	0.174
	7.97	84.745	84.874	0.130	89.416	89.293	0.123
	9.96	84.701	84.637	0.064	89.316	89.243	0.073
5	1.99	84.760	84.511	0.250	89.269	89.162	0.107
	3.98	84.704	84.464	0.240	89.276	89.080	0.196
	6.04	84.648	84.397	0.251	89.176	88.998	0.178
	7.97	84.591	84.312	0.280	89.129	88.916	0.213
	9.96	84.535	84.301	0.234	89.082	88.834	0.248

4 CONCLUSIONS

In this paper, an acceptable method for efficiency estimation of induction motors operating with non-sinusoidal voltage supply is proposed. The algorithm uses the CSO algorithm to estimate the fundamental and harmonics equivalent circuit parameters under field operating conditions while the motor is still in service. Variations of the motor parameters due to harmonics and skin effects are also considered. It was observed that the motor parameters remain fairly constant at different operating points, hence, it is enough to extract the parameters using measurements from a single operating point. Furthermore, the parameter estimation results confirm the dependence of the rotor and core loss resistances on the harmonics' order which highlight the need to estimate these parameters separately using the harmonics equivalent circuits. Although the results based on the segregation of loss method show that the additional harmonic losses are independent of load, the trend in the losses indicate noticeable dependence on the order of the harmonics. An appreciable increase in the harmonic losses has been observed in the case of the 5^{th} order harmonic and the trend tend to reduce for higher order harmonics. In terms of accuracy, the results for the balanced case indicate that the maximum absolute efficiency error for both motors at 9.96% THD_v was found to be 0.248%. This value confirms the accuracy of the proposed method. For unbalanced case, it has been observed that the efficiencies of the tested motors drop significantly due to the combined impact of the voltage unbalance and harmonic distortions of the supply. The proposed method provides results with acceptable accuracies as the maximum absolute errors of 0.3886% and 0.2480% were obtained for the 7.5kW and 37kW motors respectively.

REFERENCES

1. Liang, X. and Luy, Y. (2006). Harmonic Analysis for Induction Motors. *Canadian Conference on Electrical and Computer Engineering*, pp. 8-14.

2. Sen, P.C. (1997). Princple of Electric Machines and Power Electronics. *John Wiley and Sons, Second Ed.*, pp. 270-271.

3. Lee, S., Kim, J., Ana, D. and Hong, J. (2014). Equivalent Circuit Considering the Harmonics of Core Loss in the Squirrel-Cage Induction Motor for Electrical Power Steering Application. *IEEE Trans. Magn.*, vol. 50, no. 11, pp. 1-4.

4. Melfi, M.J. (2011). Quantifying the Energy Efficiency of Motors on Inverters. *IEEE Industry Applications Magazine*, pp. 37-43.

5. Lu, B., Habetler, T.G. and Harley, R.G. (2015). A Survey of Efficiency-Estimation Methods for In-Service Induction Motors, pp. 16-21.

6. Al-Badri, M., Pillay, P. and Angers, P. (2017). A Novel in Situ Efficiency Estimation Algorithm for Three-Phase Induction Motors Operating with Distorted Unbalanced Voltages, *IEEE Trans. Ind. Appl.*, vol. 53, no. 6, pp. 5338-5347.

7. Phumiphak, P. (2008). Nonintrusive method for estimating field efficiency of inverter-fed induction motor using measured values, *2008 IEEE Int. Conf. Sustain. Energy Technol.*, pp. 580-583.

8. Chirindo, M., Khan, M.A. and Barendse, P.S. (2016). Considerations for Nonintrusive Efficiency Estimation of Inverter-Fed Induction Motors, *IEEE Trans. Ind. Electron.*, vol. 63, no. 2, pp. 741-749.

9. Lee, S.J., Kim, S.I. and Hong, J.P. (2011). A study on characteristics of PM synchronous motors according to pole slot combinations for EPS application. *Proceedings, Compumag*, pp. 24-28.

10. IEEE Standard Test Procedure for Polyphase Induction Motors and Generators (2017). *IEEE Stand. 112-2017*, pp. 58-99.

11. IEC 60034-2-1 (2014). Standard methods for determining losses and efficiency from tests (excluding machines for traction vehicles), pp. 19-38.

12. Agamloh, E.B., Peele, S. and Grappe, J. (2017). Operation of Variable-Frequency Drive Motor Systems With Source Voltage Unbalance, vol. 53, no. 6, pp. 6038-6046.